

Figure 1

Publication	PFCVD Reaction	'Delta-n' Control Method	Post-deposition Thermal Treatment (°C/h)
Valette S., 1987	Unknown	P doping	Not specified
Valette S., 1988	Unknown	P doping	400°C
Grand G., 1990	Unknown	P doping	1000°C
Liu K., 1995	Unknown	Content in Si, P	Not specified
Ojha S., 1998	Unknown	Ge, B, or P doping	Not specified
Canning J., 1998	Unknown	Ge doping	Not specified
Bulla D., 1998	TEOS	TEOS	Not specified
Johnson C., 1998	$\text{SiH}_4 + \text{O}_2$	Si ion Implantation	400°C
Boswell R. W., 1997	$\text{SiH}_4 + \text{O}_2$	$\text{SiH}_4/\text{O}_2$ flow ratio	1000°C
Bazylenko M. V., 1995	$\text{SiH}_4 + \text{O}_2 + \text{CF}_4$	$(\text{SiH}_4/\text{O}_2)/\text{CF}_4$ flow ratio	Not specified
Bazylenko M. V., 1996	$\text{SiH}_4 + \text{O}_2 + \text{CF}_4$	$(\text{SiH}_4/\text{O}_2)/\text{CF}_4$ flow ratio	1000°C
Durand et A., 1996	$\text{SiH}_4 + \text{O}_2 + \text{CF}_4$	$\text{SiH}_4/\text{O}_2/\text{CF}_4$ flow ratio	100°C
Kasper K., 1991	$\text{SiH}_4 + \text{N}_2\text{O}$	$\text{SiH}_4/\text{N}_2\text{O}$ flow ratio	1060°C
Lai Q., 1992	$\text{SiH}_4 + \text{N}_2\text{O}$	$\text{SiH}_4/\text{N}_2\text{O}$ flow ratio	1100°C
Lai Q., 1993	$\text{SiH}_4 + \text{N}_2\text{O}$	$\text{SiH}_4/\text{N}_2\text{O}$ flow ratio	1100°C
Pereyra L., 1997	$\text{SiH}_4 + \text{N}_2\text{O}$	$\text{SiH}_4/\text{N}_2\text{O}$ flow ratio	400°C
Alayo M., 1998	$\text{SiH}_4 + \text{N}_2\text{O}$	$\text{SiH}_4/\text{N}_2\text{O}$ flow ratio	1000°C
Kenyon T., 1997	$\text{SiH}_4 + \text{N}_2\text{O} + \text{Ar}$	$\text{SiH}_4/\text{N}_2\text{O}/\text{Ar}$ flow ratio	1000°C
Lam D. K. W., 1984	$\text{SiH}_4 + \text{N}_2\text{O} + \text{NH}_3$	$\text{SiH}_4/\text{N}_2\text{O}/\text{NH}_3$ flow ratio	Not specified
Bruno F., 1991	$\text{SiH}_4 + \text{N}_2\text{O} + \text{NH}_3$	$\text{SiH}_4/\text{N}_2\text{O}/\text{NH}_3$ flow ratio	1100°C
Yokohama S., 1995	$\text{SiH}_4 + \text{N}_2\text{O} + \text{NH}_3$	$\text{SiH}_4/\text{N}_2\text{O}/\text{NH}_3$ flow ratio	Not specified
Agnihotri O. P., 1997	$\text{SiH}_4 + \text{N}_2\text{O} + \text{NH}_3$	$\text{SiH}_4/\text{N}_2\text{O}/\text{NH}_3$ flow ratio	700-900°C
Germann R., 1999	$\text{SiH}_4 + \text{N}_2\text{O} + \text{NH}_3$	Unknown	1100°C
Offrein B., 1999	$\text{SiH}_4 + \text{N}_2\text{O} + \text{NH}_3$	Unknown	1150°C
Hoffmann M., 1995	$\text{SiH}_4 + \text{N}_2\text{O} + \text{NH}_3 + \text{Ar}$	$\text{SiH}_4/\text{N}_2\text{O}/\text{NH}_3/\text{Ar}$ flow ratio	Not specified
Hoffmann M., 1997	$\text{SiH}_4 + \text{N}_2\text{O} + \text{NH}_3 + \text{Ar}$	$\text{SiH}_4/\text{N}_2\text{O}/\text{NH}_3/\text{Ar}$ flow ratio	Not specified
Tu Y., 1995	$\text{SiH}_4 + \text{N}_2\text{O} + \text{NH}_3 + \text{N}_2$	$\text{N}_2\text{O}/(\text{N}_2\text{O} + \text{NH}_3)$ flow ratio	1050°C
Poenar D., 1997	$\text{SiH}_4 + \text{N}_2\text{O} + \text{NH}_3 + \text{N}_2$	$\text{SiH}_4/\text{N}_2\text{O}/\text{NH}_3/\text{N}_2$ flow ratio	850°C
Ridder R., 1998	$\text{SiH}_4 + \text{N}_2\text{O} + \text{NH}_3 + \text{N}_2$	$\text{SiH}_4/\text{N}_2\text{O}/\text{NH}_3/\text{Ar}$ flow ratio	1100°C
Worhoff K., 1999	$\text{SiH}_4 + \text{N}_2\text{O} + \text{NH}_3 + \text{N}_2$	$\text{SiH}_4/\text{N}_2\text{O}/\text{NH}_3/\text{N}_2$ flow ratio	1150°C
Bulat E.S., 1993	$\text{SiH}_4 + \text{N}_2\text{O} + \text{N}_2 + \text{O}_2 + \text{He} + \text{CF}_4$	$\text{SiH}_4/(\text{N}_2\text{O}/\text{N}_2)/\text{O}_2/\text{CF}_4$ flow ratio	425°C
This Patent Application	$\text{SiH}_4 + \text{N}_2\text{O} + \text{PH}_3 + \text{N}_2$	Patented Pending Method	650°C

Figure 2

			HO-H	SiOH	SiNH	SiNH	SiH	Si-O	N-N	Si-O-Si	SiO-Si	SiON	SiOH	SiO-Si	SiO-Si
FTIR	1st mode (cm <sup>-1</sup> )	Min	3550	3470	3380	3300	2210	1800	1530	1080	1000	910	860	740	410
		Ave	3650	3510	3420	3380	2260	1875	1555	1180	1080	950	885	810	460
		Max	3750	3550	3460	3460	2310	1950	1580	1280	1160	990	910	880	510
1st mode (μm)	Min	2.817	2.882	2.959	3.030	4.525	5.556	6.536	9.259	10.000	10.989	11.628	13.514	24.390	
	Ave	2.740	2.849	2.924	2.959	4.425	5.333	6.431	8.475	9.259	10.526	11.299	12.346	21.739	
	Max	2.667	2.817	2.890	2.890	4.329	5.128	6.329	7.813	8.621	10.101	10.989	11.364	19.608	
2nd mode (μm)	Min	1.408	1.441	1.479	1.515	2.262	2.778	3.268	4.630	5.000	5.495	5.814	6.757	12.195	
	Ave	1.370	1.425	1.462	1.479	2.212	2.667	3.215	4.237	4.630	5.263	5.650	6.173	10.870	
	Max	1.333	1.408	1.445	1.445	2.165	2.564	3.165	3.906	4.310	5.051	5.495	5.682	9.804	
3rd mode (μm)	Min	0.939	0.961	0.986	1.010	1.508	1.852	2.179	3.086	3.333	3.663	3.876	4.505	8.130	
	Ave	0.913	0.950	0.975	0.986	1.475	1.778	2.144	2.825	3.086	3.509	3.766	4.115	7.246	
	Max	0.889	0.939	0.963	0.963	1.443	1.709	2.110	2.604	2.874	3.367	3.663	3.788	6.536	
4th mode (μm)	Min	0.704	0.720	0.740	0.758	1.131	1.389	1.634	2.315	2.500	2.747	2.907	3.378	6.098	
	Ave	0.685	0.712	0.731	0.740	1.106	1.333	1.608	2.119	2.315	2.632	2.825	3.086	5.435	
	Max	0.667	0.704	0.723	0.723	1.082	1.282	1.582	1.953	2.155	2.525	2.747	2.841	4.902	
5th mode (μm)	Min	0.563	0.576	0.592	0.606	0.905	1.111	1.307	1.852	2.000	2.198	2.326	2.703	4.878	
	Ave	0.548	0.570	0.585	0.592	0.885	1.067	1.286	1.695	1.852	2.105	2.260	2.469	4.348	
	Max	0.533	0.563	0.578	0.578	0.866	1.026	1.266	1.563	1.724	2.020	2.198	2.273	3.922	
6th mode (μm)	Min	0.469	0.480	0.493	0.505	0.754	0.926	1.089	1.543	1.667	1.832	1.938	2.252	4.065	
	Ave	0.457	0.475	0.487	0.493	0.737	0.889	1.072	1.412	1.543	1.754	1.883	2.058	3.623	
	Max	0.444	0.469	0.482	0.482	0.722	0.855	1.055	1.302	1.437	1.684	1.832	1.894	3.268	
7th mode (μm)	Min	0.402	0.412	0.423	0.433	0.646	0.794	0.934	1.323	1.429	1.570	1.661	1.931	3.484	
	Ave	0.391	0.407	0.418	0.423	0.632	0.762	0.919	1.211	1.323	1.504	1.614	1.764	3.106	
	Max	0.381	0.402	0.413	0.413	0.618	0.733	0.904	1.116	1.232	1.443	1.570	1.623	2.801	
8th mode (μm)	Min	0.352	0.360	0.370	0.379	0.566	0.694	0.817	1.157	1.250	1.374	1.453	1.689	3.049	
	Ave	0.342	0.356	0.365	0.370	0.553	0.667	0.804	1.059	1.157	1.316	1.412	1.543	2.717	
	Max	0.333	0.352	0.361	0.361	0.541	0.641	0.791	0.977	1.078	1.263	1.374	1.420	2.451	

Figure 3a

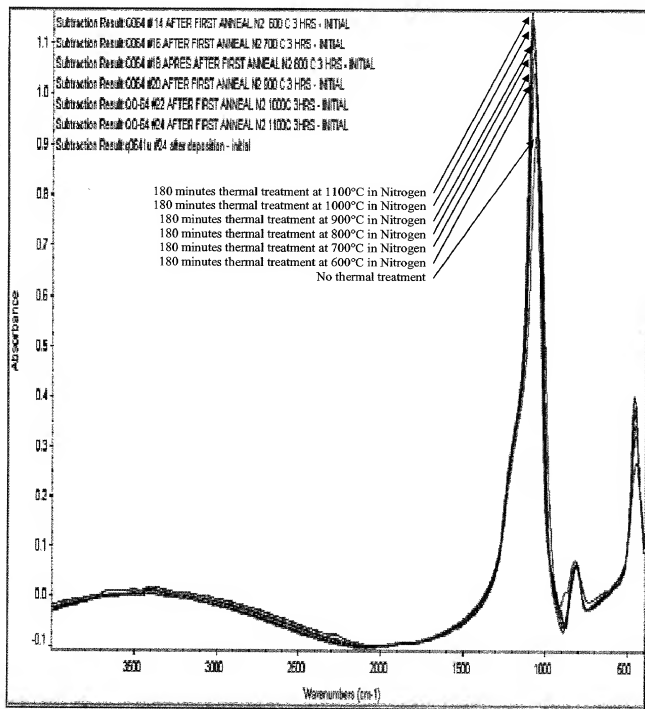


Figure 3b

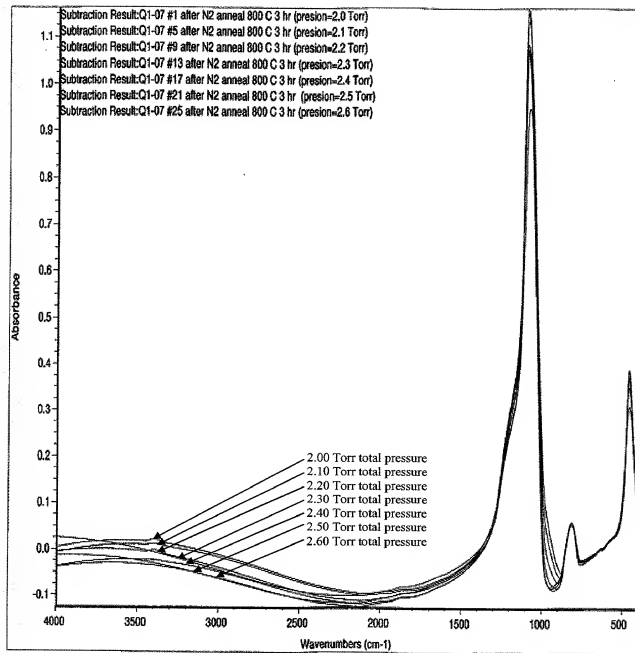


Figure 3c

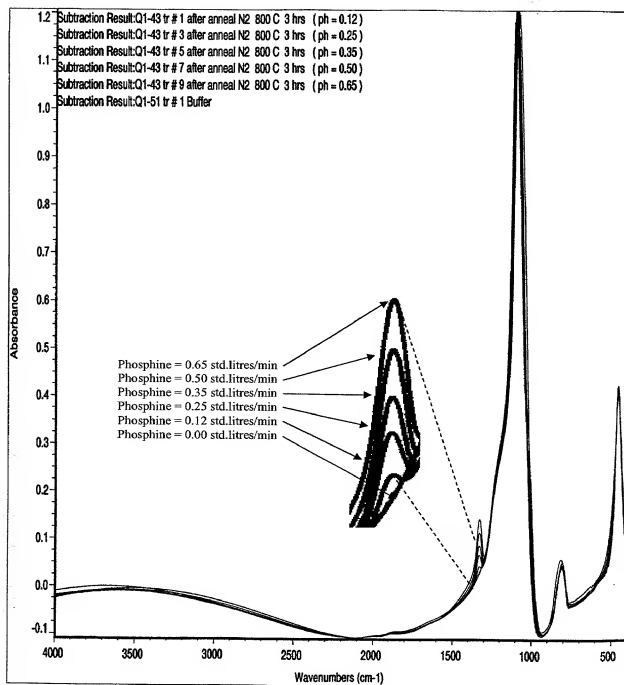


Figure 3d

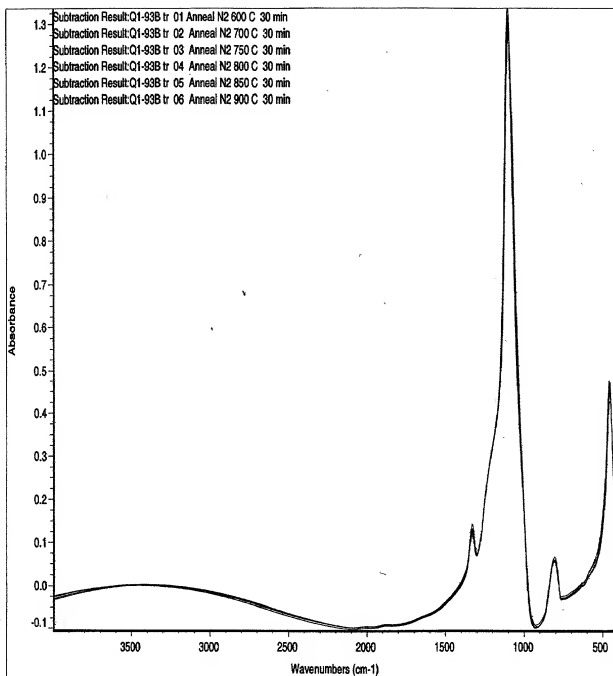
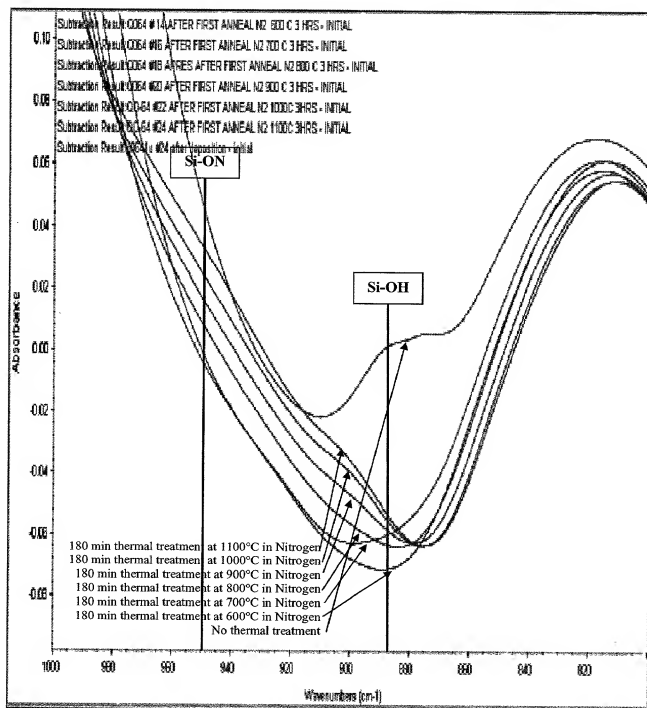


Figure 4a



00972778-000000

Figure 4b

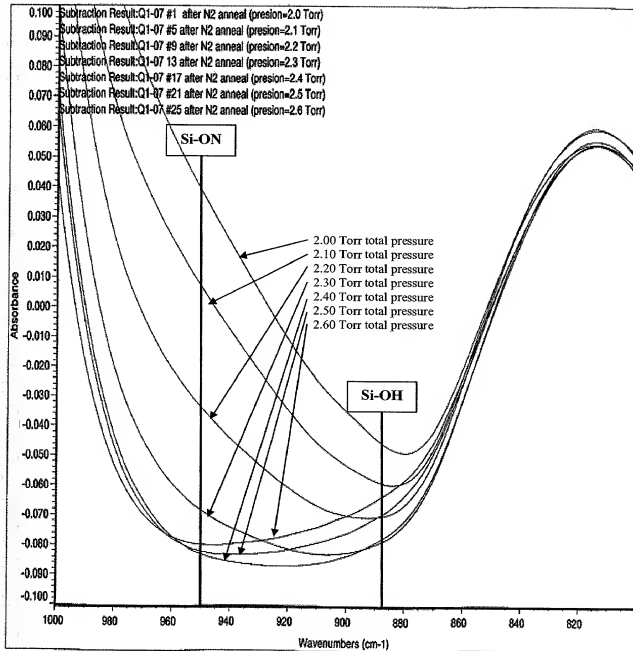




Figure 4c

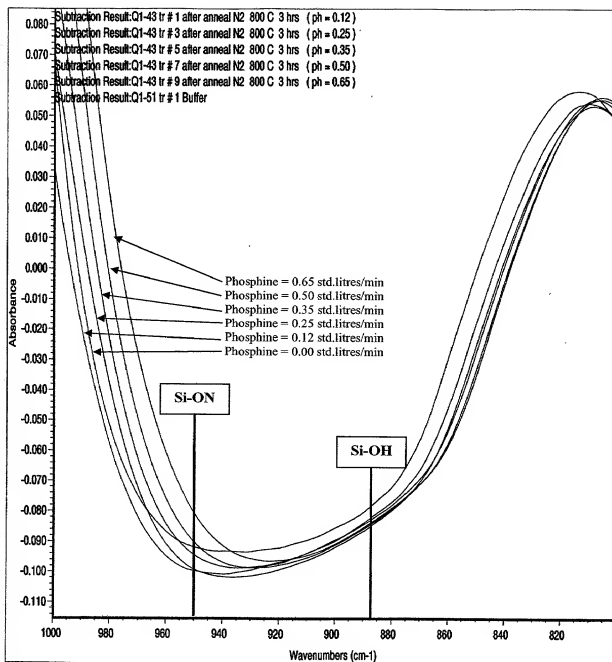


Figure 4d

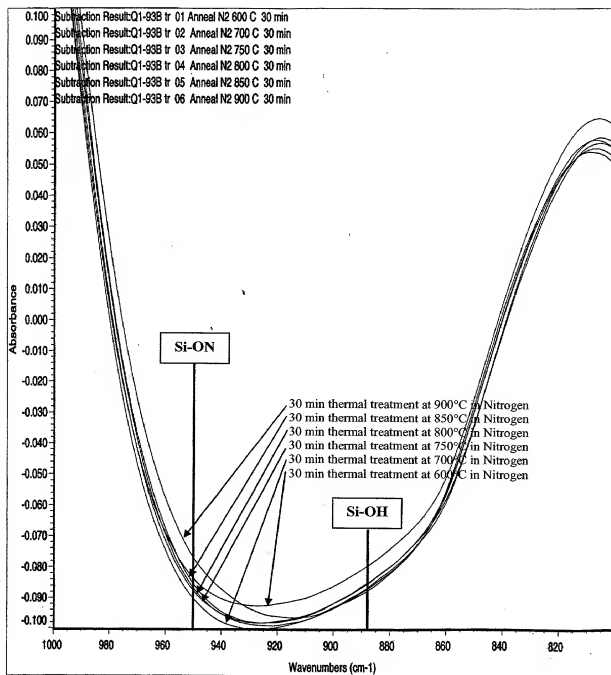


Figure 5c

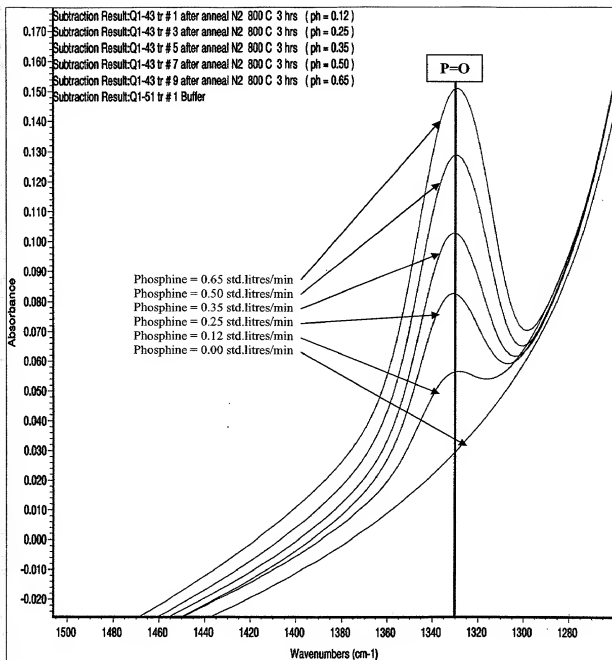


Figure 5d

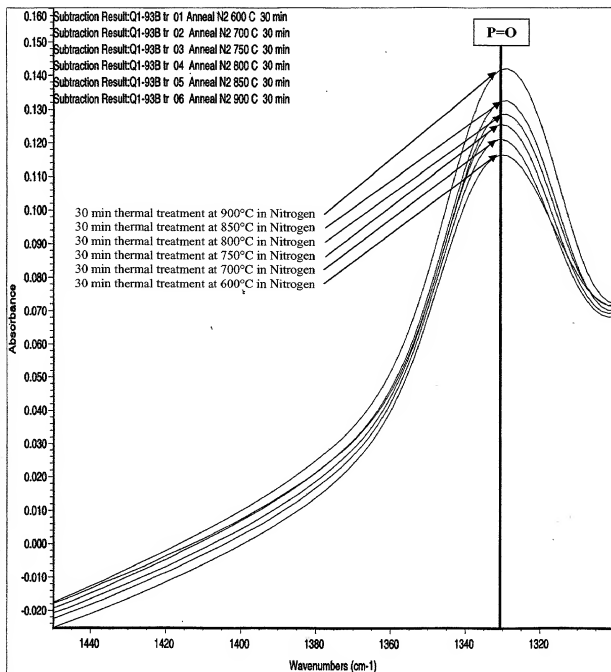


Figure 6a

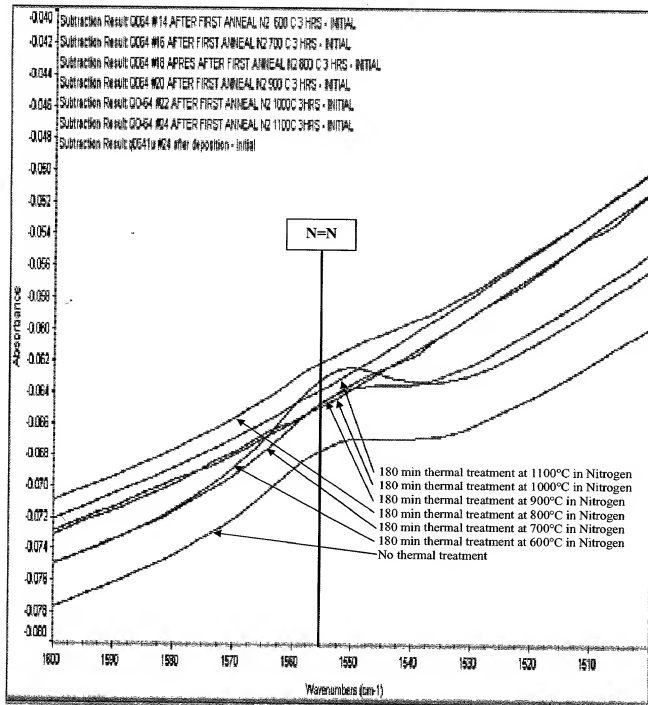


Figure 6b

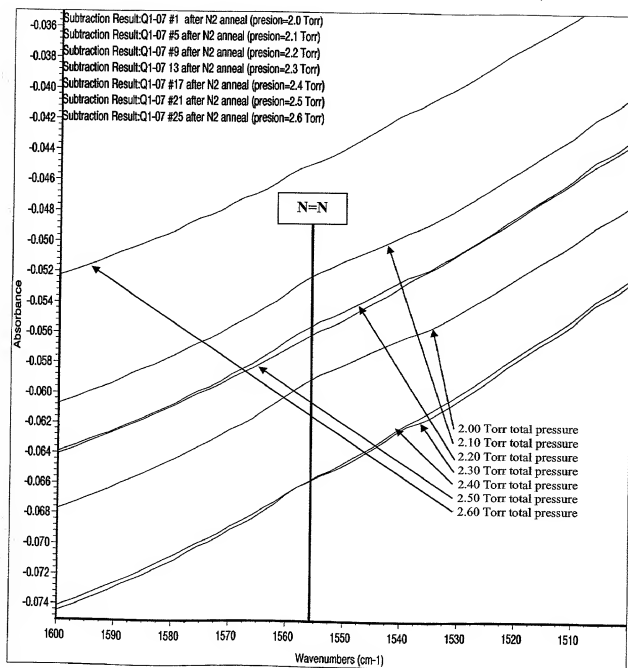


Figure 6c

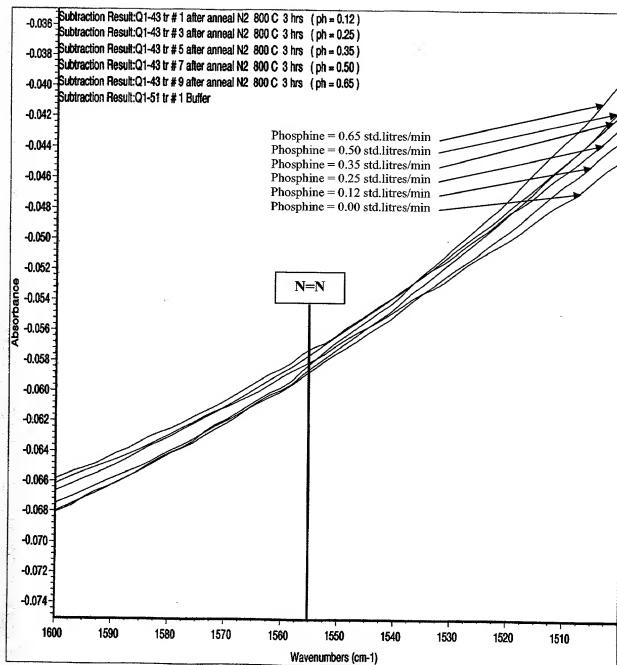


Figure 6d

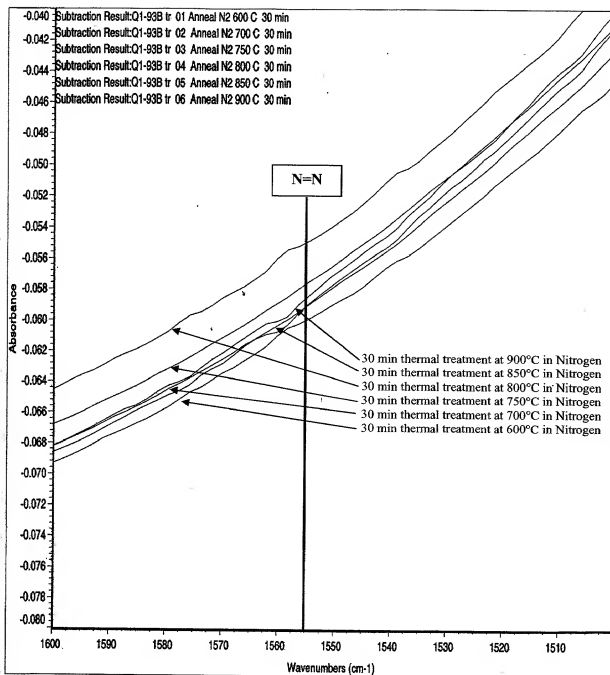




Figure 7a

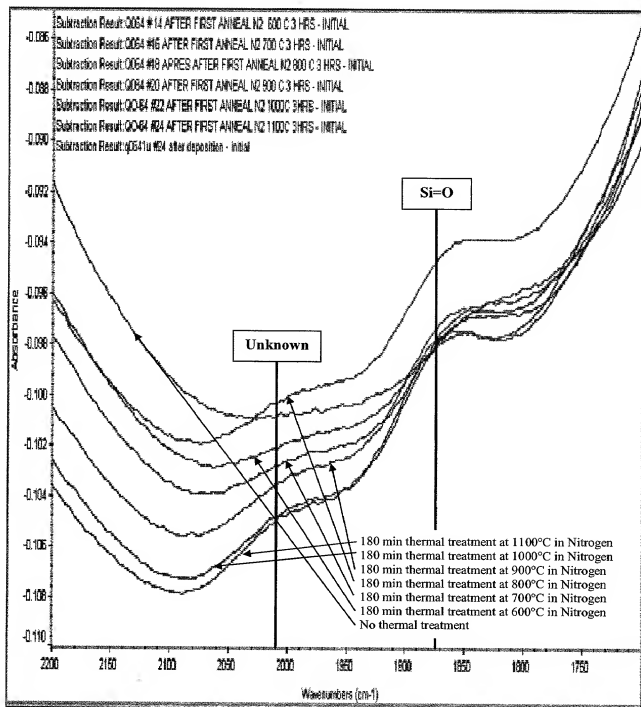


Figure 7b

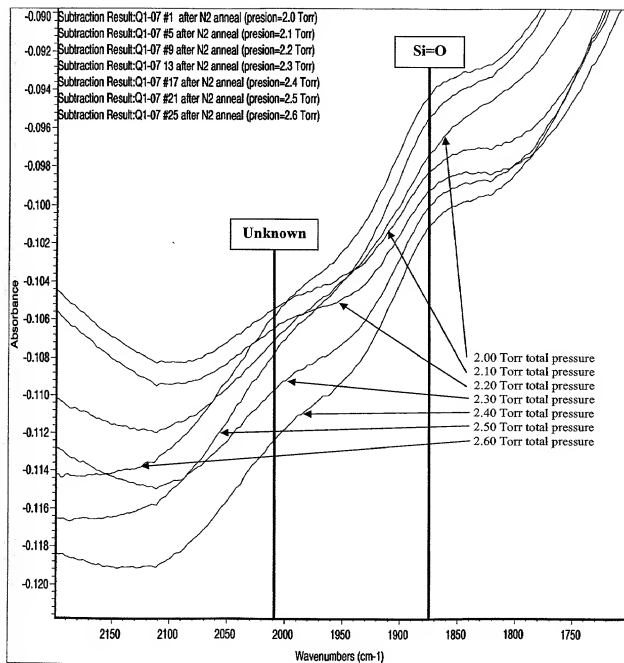


Figure 7c

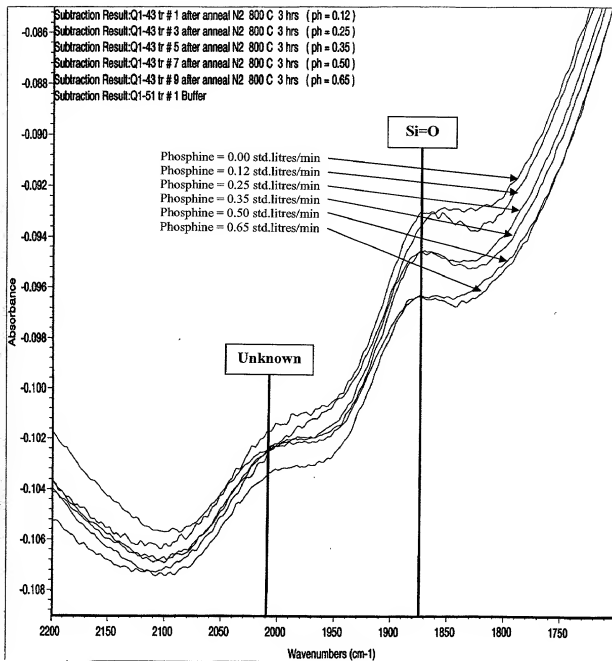


Figure 7d

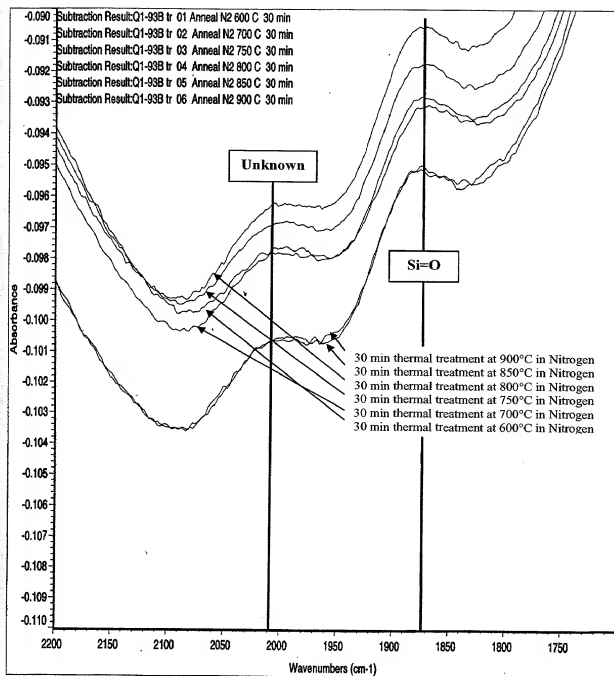


Figure 8a

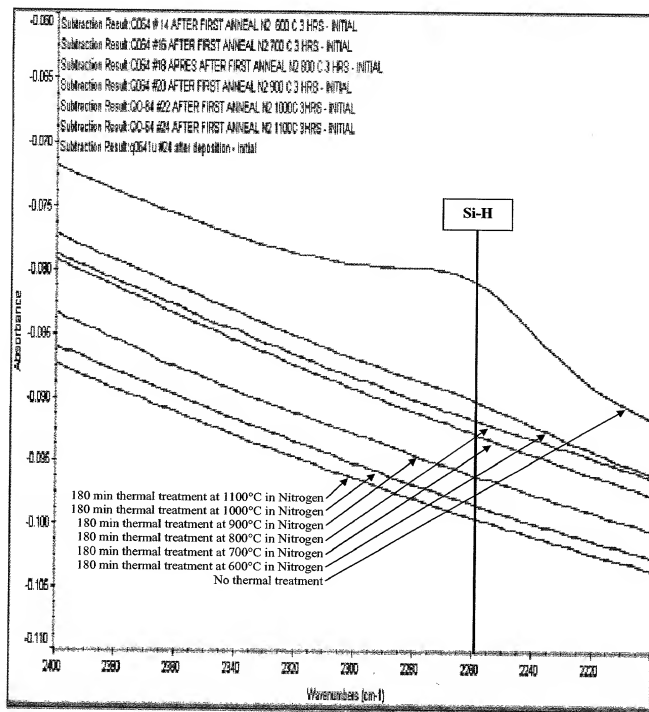


Figure 8b

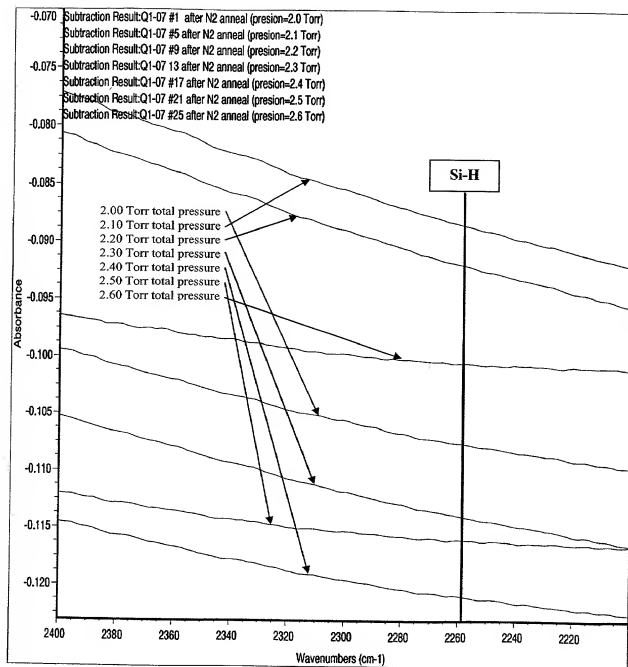


Figure 8c

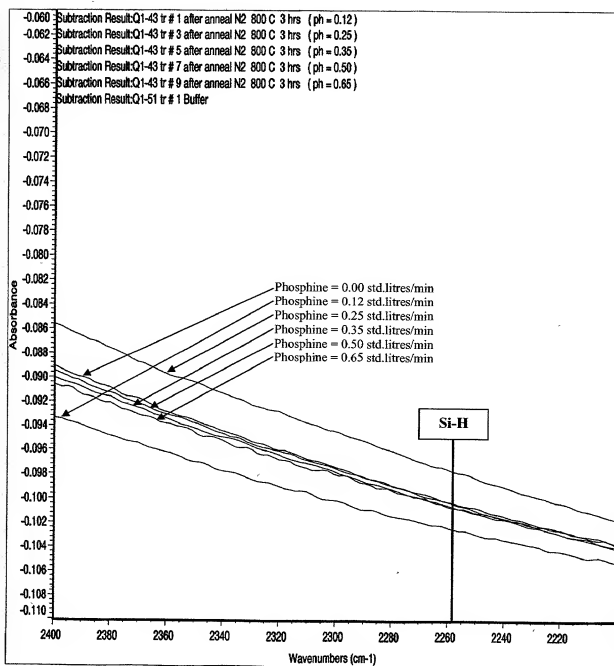


Figure 8d

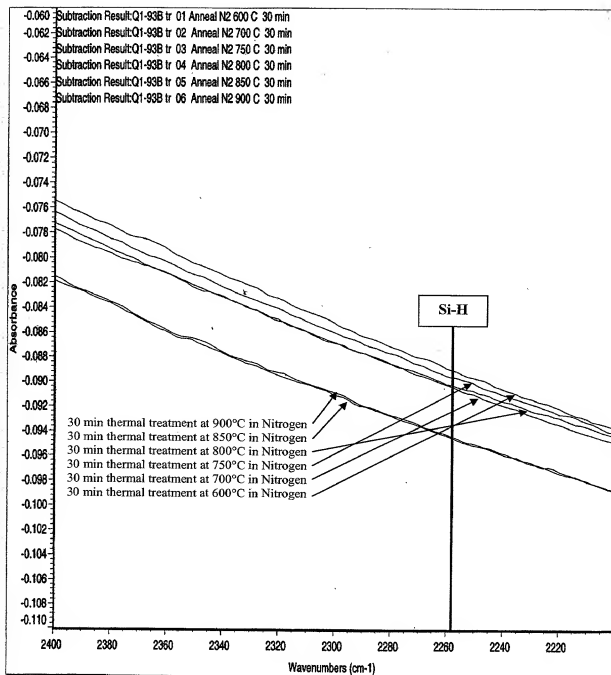




Figure 9a

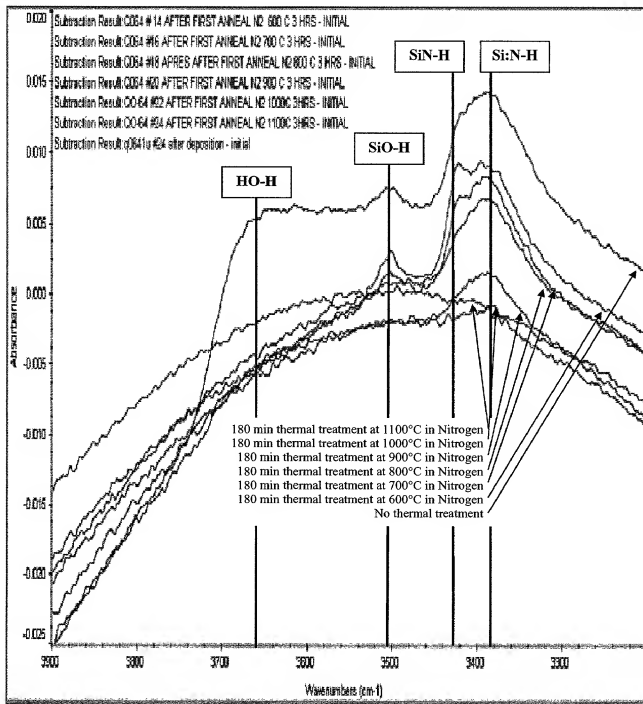


Figure 9b

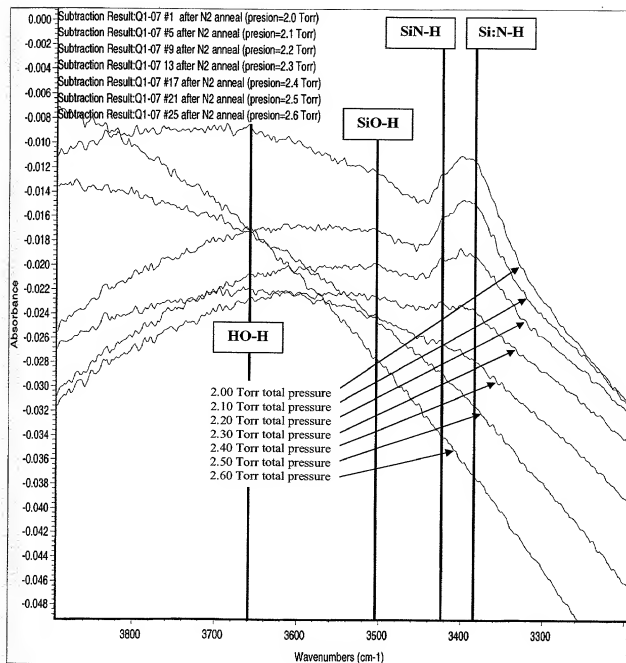


Figure 9c

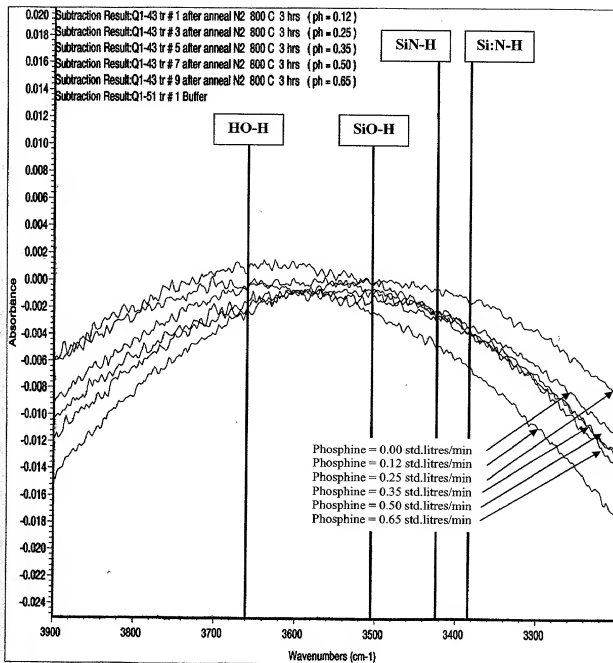


Figure 9d

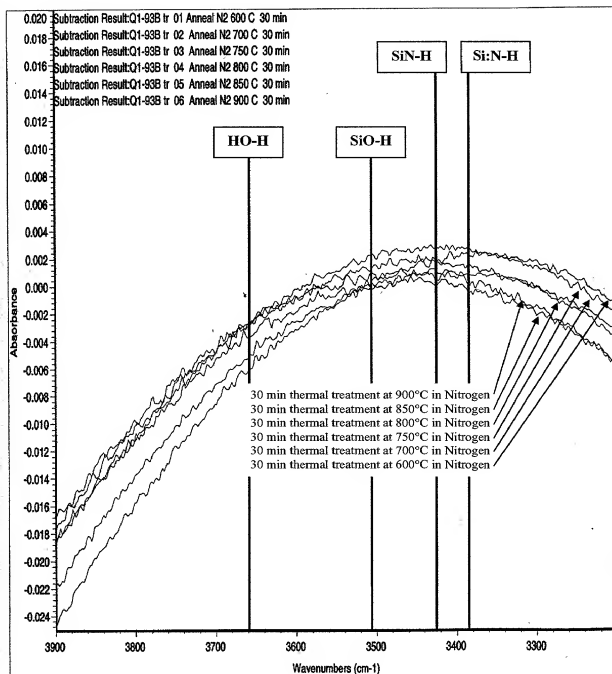
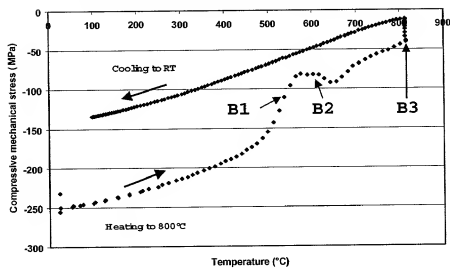


Figure 10

Buffer (Clad) compressive mechanical stress during a 180 minutes thermal treatment in a nitrogen ambient



Core tensile mechanical stress during a 180 minutes thermal treatment in a nitrogen ambient

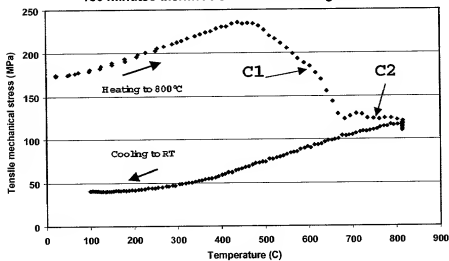


Figure 11

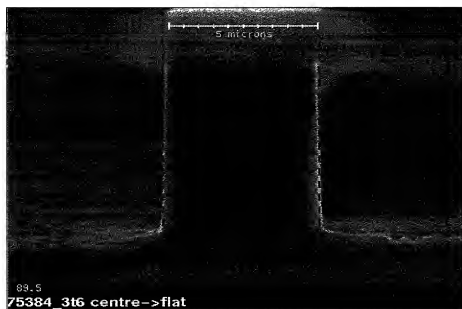
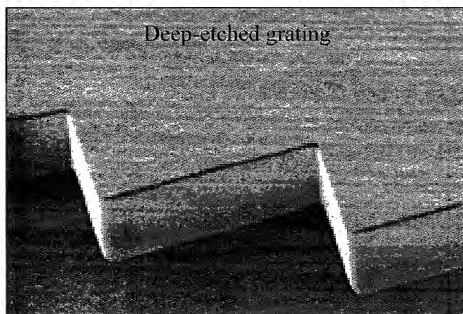
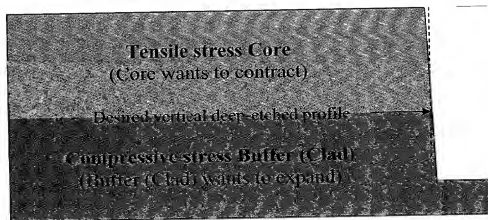
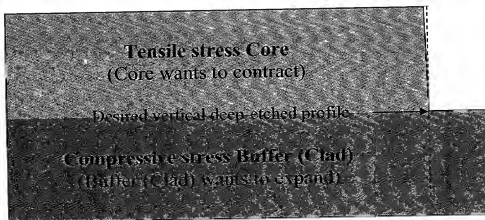
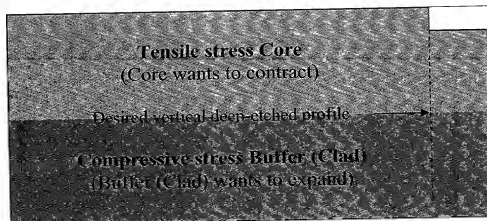
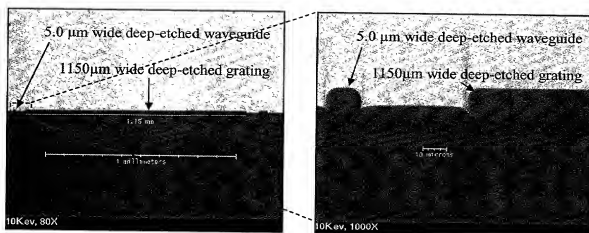


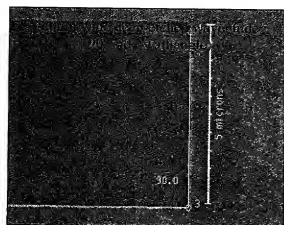
Figure 12



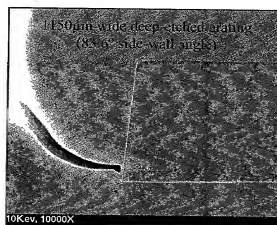
**Figure 13**



The relative position between an isolated 5.0 $\mu$ m wide deep-etched waveguide and its neighboring 1150 $\mu$ m wide deep-etched grating at two different magnifications.



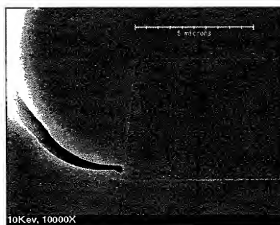
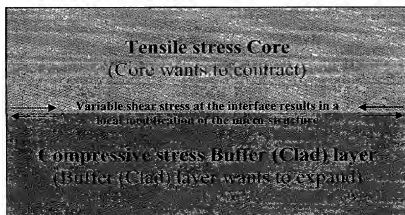
The side-wall of the 5.0 $\mu$ m wide deep-etched waveguide facing the neighboring grating has a slope of about 90°.

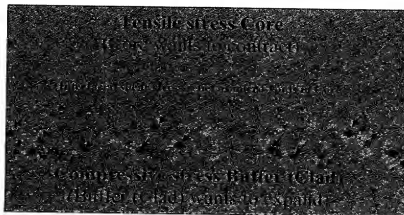
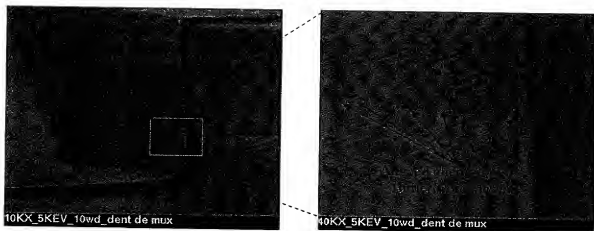


The side-wall of the 1150 $\mu$ m wide deep-etched grating facing the neighboring deep-etched waveguide has a much smaller slope of about 84°.

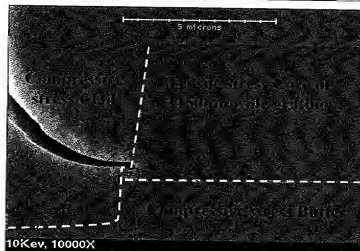


Figure 14



[illegible]

**Figure 16**



## Conclusion

10Key, 10000X

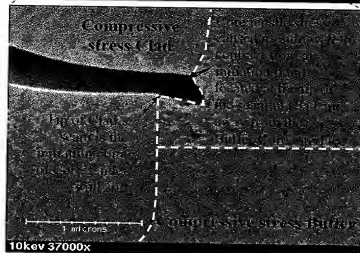


Fig. 1. Clay  
Seal is the  
material that  
locks the  
door shut.

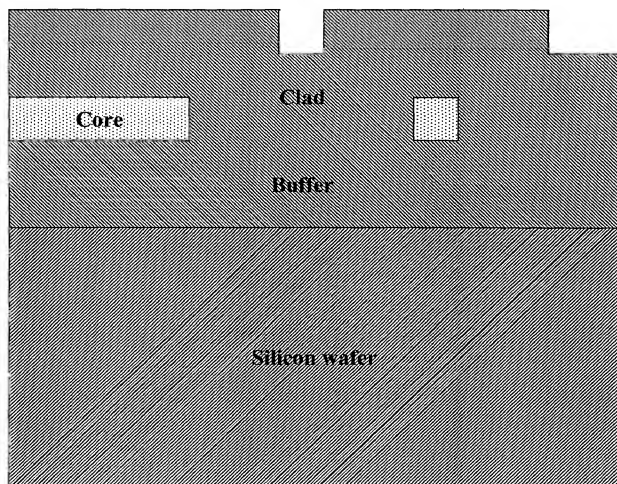
1991-1992

### Impressive Stress Buildup

10kev 37000x

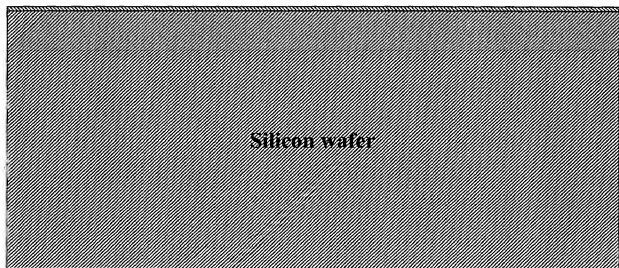
	0	1	2	3	4	5	6	7	8	9	10	11	12	13	14	15	16	17	18	19	20	21	22	23	24	25	26	27	28	29	30	31	32	33	34	35	36	37	38	39	40	41	42	43	44	45	46	47	48	49	50	51	52	53	54	55	56	57	58	59	60	61	62	63	64	65	66	67	68	69	70	71	72	73	74	75	76	77	78	79	80	81	82	83	84	85	86	87	88	89	90	91	92	93	94	95	96	97	98	99	100
0	0	1	2	3	4	5	6	7	8	9	10	11	12	13	14	15	16	17	18	19	20	21	22	23	24	25	26	27	28	29	30	31	32	33	34	35	36	37	38	39	40	41	42	43	44	45	46	47	48	49	50	51	52	53	54	55	56	57	58	59	60	61	62	63	64	65	66	67	68	69	70	71	72	73	74	75	76	77	78	79	80	81	82	83	84	85	86	87	88	89	90	91	92	93	94	95	96	97	98	99	100

Figure 17

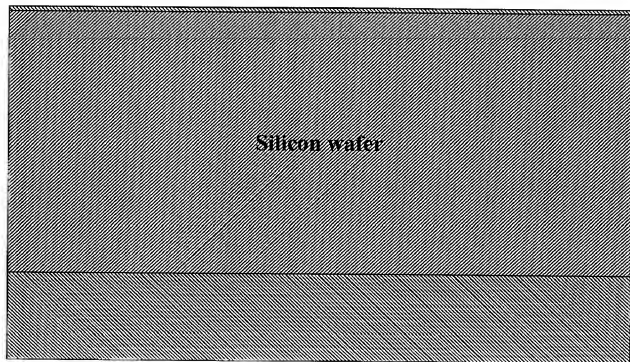


00973779-020502

**Figure 18a**

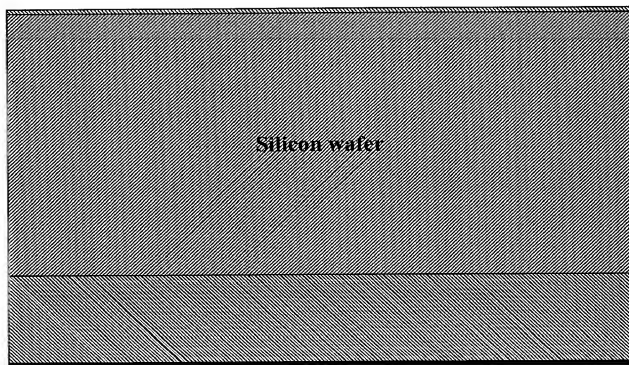
[illegible]

**Figure 18b**



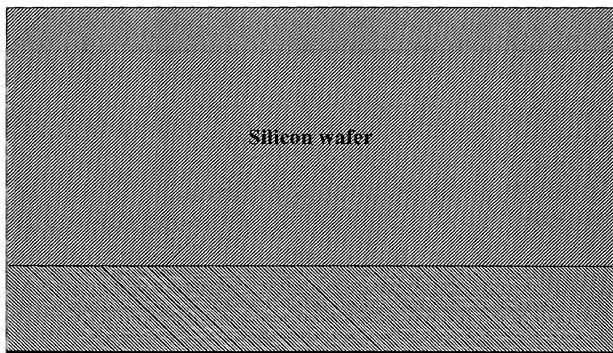
000000-000000

Figure 18c



Silicon wafer

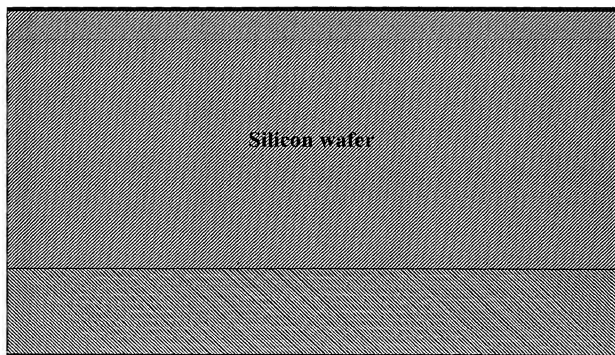
**Figure 18d**



00073779.000502

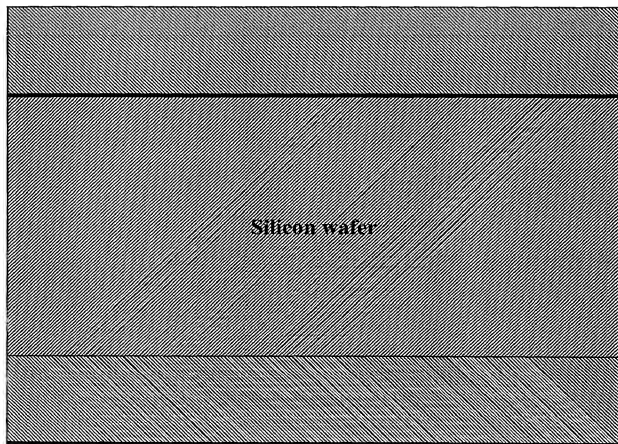


Figure 18e



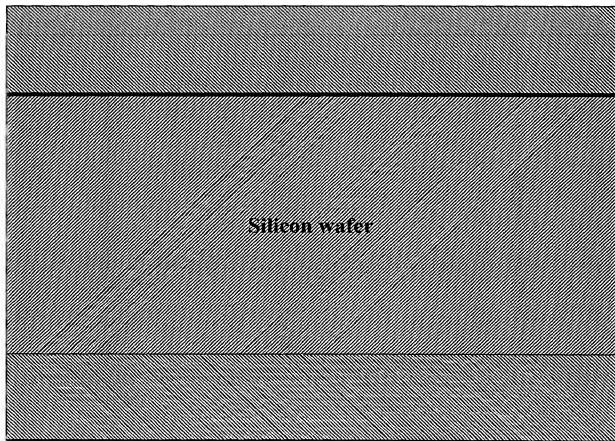
00072779.000002

Figure 18f



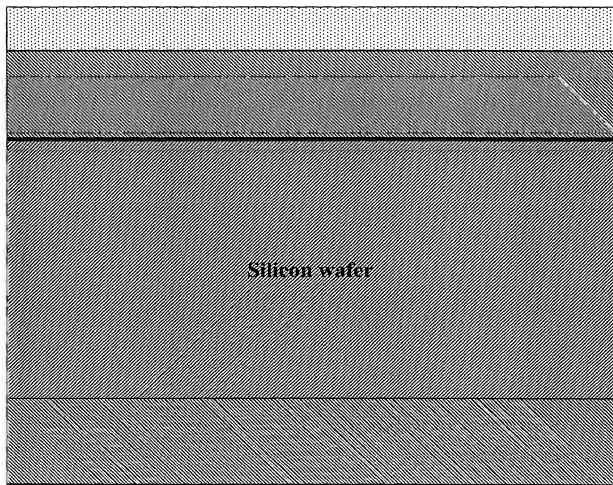
09973779.020502

Figure 18g



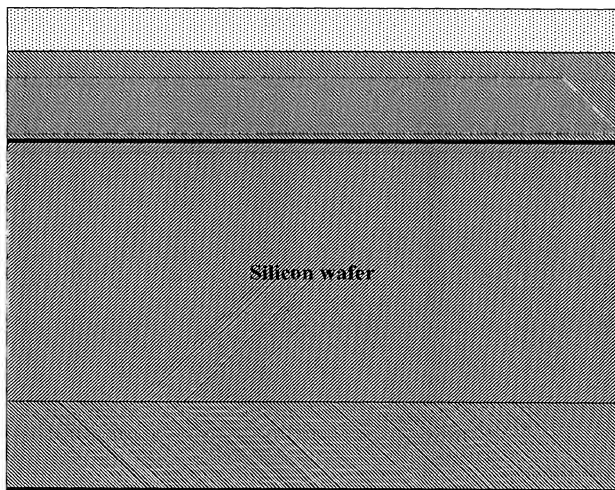
00072779.000802

Figure 18h



00973779-020602

Figure 18i



09973779-020502

Figure 18j

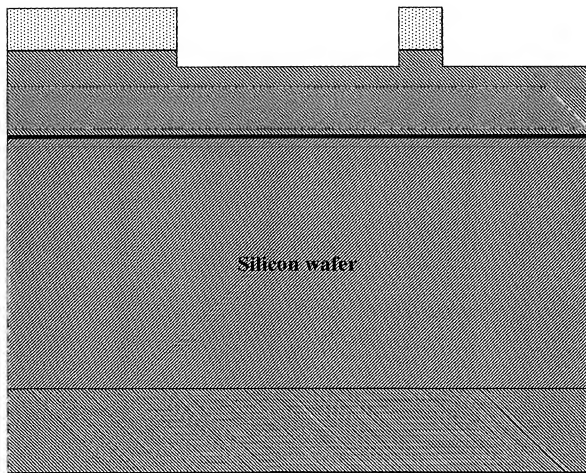
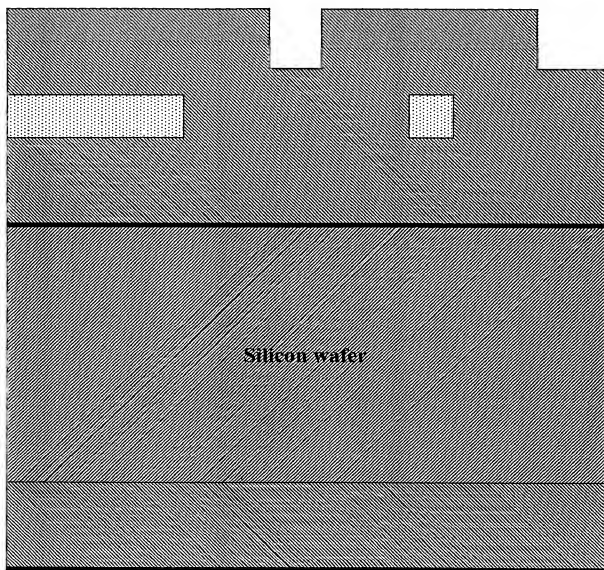
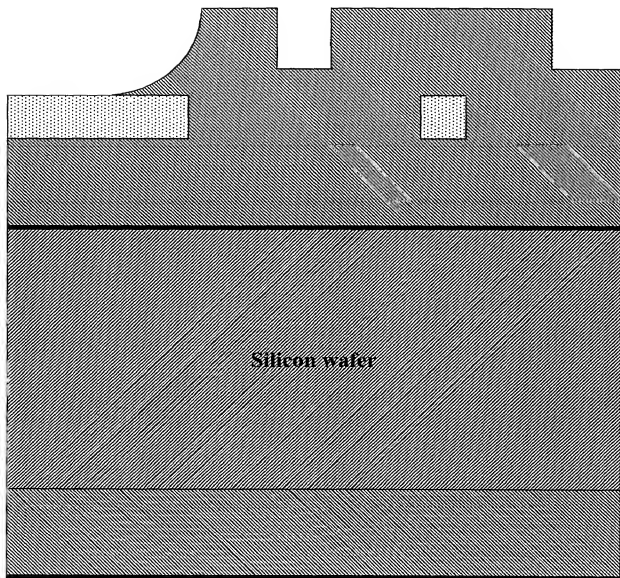


Figure 18k



00072779-020500

Figure 181



09072728-000002



Figure 19

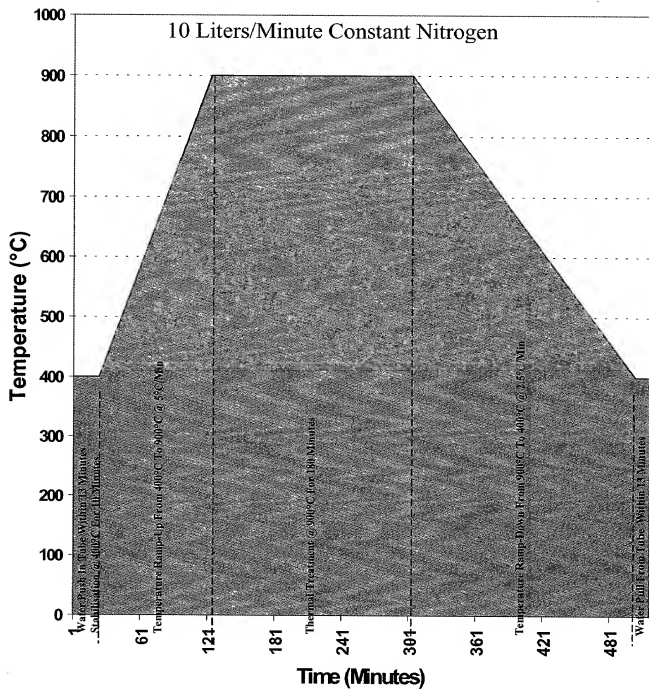
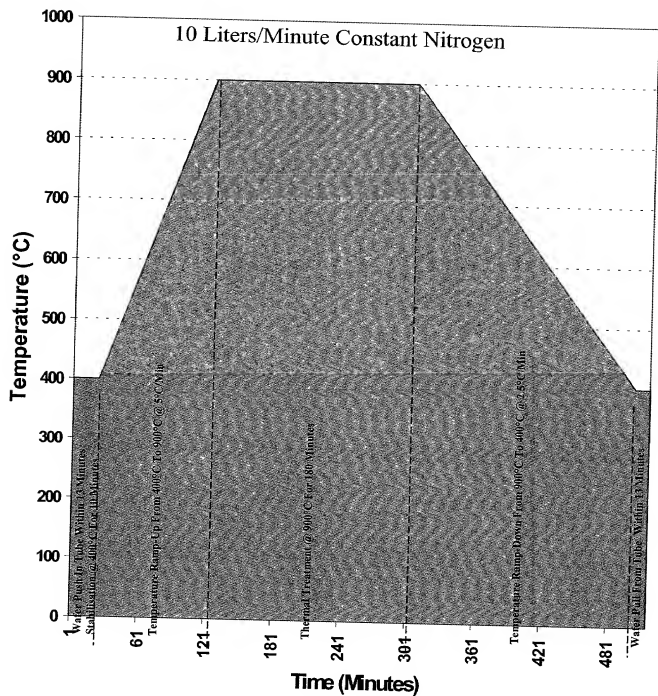


Figure 20



**Figure 21**



Figure 22

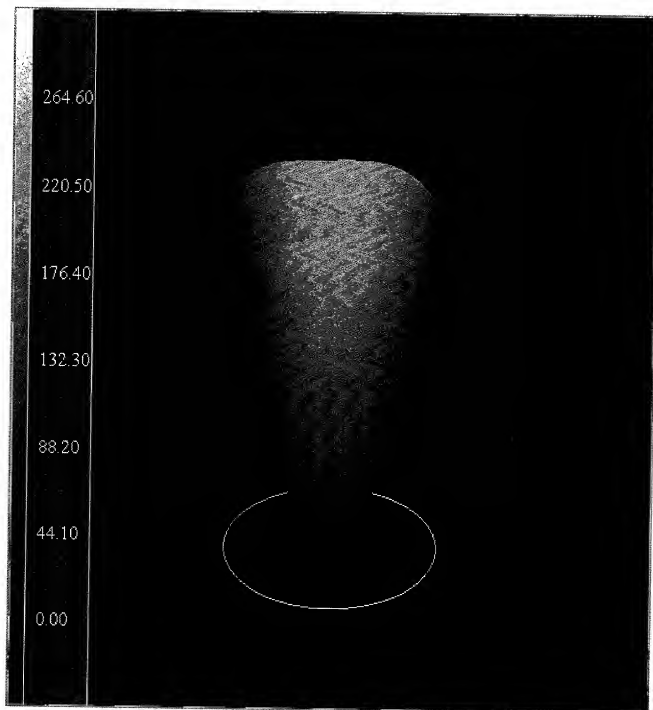


**Figure 23**

